

# Inhibition of a TREK-like $K^+$ channel current by noradrenaline requires both $\beta_1$ - and $\beta_2$ -adrenoceptors in rat atrial myocytes

Richard C. Bond, Stéphanie C.M. Choisy, Simon M. Bryant, Jules C. Hancox, and Andrew F. James\*

Bristol Cardiovascular Research Laboratories, School of Physiology and Pharmacology, University of Bristol, Medical Sciences Building, University Walk, Bristol BS8 1TD, UK

Received 4 June 2013; revised 21 July 2014; accepted 30 July 2014

Time for primary review: 45 days

<b>Aims</b>	Noradrenaline plays an important role in the modulation of atrial electrophysiology. However, the identity of the modulated channels, their mechanisms of modulation, and their role in the action potential remain unclear. This study aimed to investigate the noradrenergic modulation of an atrial steady-state outward current ( $I_{Kss}$ ).
<b>Methods and results</b>	Rat atrial myocyte whole-cell currents were recorded at 36°C. Noradrenaline potently inhibited $I_{Kss}$ ( $IC_{50} = 0.90$ nM, $42.1 \pm 4.3\%$ at 1 $\mu$ M, $n = 7$ ) and potentiated the L-type $Ca^{2+}$ current ( $I_{CaL}$ , $EC_{50} = 136$ nM, $205 \pm 40\%$ at 1 $\mu$ M, $n = 6$ ). Noradrenaline-sensitive $I_{Kss}$ was weakly voltage-dependent, time-independent, and potentiated by the arachidonic acid analogue, 5,8,11,14-eicosatetraynoic acid (EYTA; 10 $\mu$ M), or by osmotically induced membrane stretch. Noise analysis revealed a unitary conductance of $8.4 \pm 0.42$ pS ( $n = 8$ ). The biophysical/pharmacological properties of $I_{Kss}$ indicate a TREK-like $K^+$ channel. The effect of noradrenaline on $I_{Kss}$ was abolished by combined $\beta_1$ -/ $\beta_2$ -adrenoceptor antagonism (1 $\mu$ M propranolol or 10 $\mu$ M $\beta_1$ -selective atenolol and 100 nM $\beta_2$ -selective ICI-118,551 in combination), but not by $\beta_1$ - or $\beta_2$ -antagonist alone. The action of noradrenaline could be mimicked by $\beta_2$ -agonists (zinterol and fenoterol) in the presence of $\beta_1$ -antagonist. The action of noradrenaline on $I_{Kss}$ , but not on $I_{CaL}$ , was abolished by pertussis toxin (PTX) treatment. The action of noradrenaline on $I_{CaL}$ was mediated by $\beta_1$ -adrenoceptors via a PTX-insensitive pathway. Noradrenaline prolonged APD <sub>30</sub> by $52 \pm 19\%$ ( $n = 5$ ; $P < 0.05$ ), and this effect was abolished by combined $\beta_1$ -/ $\beta_2$ -antagonism, but not by atenolol alone.
<b>Conclusion</b>	Noradrenaline inhibits a rat atrial TREK-like $K^+$ channel current via a PTX-sensitive mechanism involving co-operativity of $\beta_1$ -/ $\beta_2$ -adrenoceptors that contributes to atrial APD prolongation.
<b>Keywords</b>	Background $K^+$ current • Beta-adrenoceptor • $K_{2P}$ channel • Steady-state outward current • Osmotic stretch • TREK-1 • Arachidonic acid

## 1. Introduction

Cardiac sympathetic activity plays an important role in electrophysiological responses of the atria and in the genesis of atrial tachyarrhythmias.<sup>1,2</sup> Noradrenaline is the principal neurotransmitter released from sympathetic postganglionic fibres and acts via  $\alpha_1$ -,  $\beta_1$ -, and  $\beta_2$ -adrenoceptors through multiple signalling pathways to modulate atrial ion channel and transporter function and thereby electrophysiological activity.<sup>1–3</sup> For example, the action of  $\beta$ -adrenoceptor stimulation on  $Ca^{2+}$  entry via L-type  $Ca^{2+}$  channel current ( $I_{CaL}$ ) and sarcoplasmic reticulum function underlies the positive inotropic

response to sympathetic activity and, under pathological conditions in the predisposed heart, may contribute to triggered activity through after-depolarizations and abnormal automaticity.<sup>4,5</sup> On the other hand, the effects of noradrenaline on  $K^+$  channel currents are likely to contribute changes in membrane excitability and repolarization.<sup>1,2</sup> The inwardly rectifying background  $K^+$  current ( $I_{K1}$ ) and the steady-state outward  $K^+$  current ( $I_{Kss}$ ) have been reported to be inhibited by  $\alpha_1$ - and  $\beta$ -adrenoceptor agonists<sup>6–14</sup> and may be important in the noradrenergic control of excitability, action potential (AP) profile, and refractoriness, and may thereby contribute to the arrhythmic substrate.<sup>2,15,16</sup>

\* Corresponding author. Tel: +44 117 331 2297; fax: +44 117 331 2288, Email: a.james@bristol.ac.uk

© The Author 2014. Published by Oxford University Press on behalf of the European Society of Cardiology.

This is an Open Access article distributed under the terms of the Creative Commons Attribution Non-Commercial License (<http://creativecommons.org/licenses/by-nc/4.0/>), which permits non-commercial re-use, distribution, and reproduction in any medium, provided the original work is properly cited. For commercial re-use, please contact [journals.permissions@oup.com](mailto:journals.permissions@oup.com)

However, the channels contributing to the effects of noradrenergic activation on atrial  $I_{K1}$  and  $I_{Kss}$  and the receptor/signalling pathways remain unresolved. Moreover, since many of the previous studies on  $I_{K1}$  and  $I_{Kss}$  have been conducted using receptor-selective combinations of agonists and antagonists, the net effect of the physiological agonist, noradrenaline, is often unclear.<sup>6–14</sup>  $I_{K1}$  is largely carried by inward rectifier  $K^+$  ( $K_{ir2.x}$ ) channels, although the two-pore domain  $K^+$  ( $K_{2P}$ ) channel, TWIK-1 ( $K_{2P1.1}$ ), may also contribute.<sup>16,17</sup> The inward rectifier channels,  $K_{ir3.1}$  and  $K_{ir3.4}$ , form a heteromultimeric G-protein-gated channel that underlies the current activated by acetylcholine ( $I_{KACh}$ ) via a pertussis toxin (PTX)-sensitive mechanism in atrial myocytes.<sup>16</sup> A number of  $K^+$  channels have been proposed to be involved in  $I_{Kss}$ , although the precise molecular composition of the underlying channels remains unclear. The voltage- and time-dependent kinetics of  $I_{Kss}$  are distinct from those of the delayed rectifier currents,  $I_{Kr}$  and  $I_{Ks}$ .<sup>18</sup> The lack of detectable inactivation, together with relative insensitivity to 4-aminopyridine (4-AP), distinguishes  $I_{Kss}$  from the ultra-rapidly activating delayed rectifier current ( $I_{Kur}$ ).<sup>15,19</sup> The two-pore domain  $K^+$  ( $K_{2P}$ ) channel, TREK-1 ( $K_{2P2.1}$ ), is a weakly voltage-dependent arachidonic acid- and mechano-sensitive channel expressed in the heart that is suggested to contribute to  $I_{Kss}$  and is modulated by isoprenaline in atrial myocytes.<sup>17,20–24</sup> TASK-1 ( $K_{2P3.1}$ ) is an acid-sensitive  $K_{2P}$  channel proposed to contribute to cardiac background currents and suggested to be under G-protein-coupled receptor control.<sup>25–30</sup> In addition, the six transmembrane-domain voltage-gated  $K^+$  channel, SLICK (slo2.1 or  $K_{Ca4.2}$ ), is a  $Ca^{2+}$ -independent homologue of the BK channel (slo1.1 or  $K_{Ca1.1}$ ) that is expressed in the heart and has been suggested to contribute to  $\alpha_{1A}$ -adrenoceptor-sensitive  $I_{Kss}$  in ventricular myocytes.<sup>14,31</sup>

Much of the work characterizing the properties of  $I_{Kss}$  and its modulation by adrenoceptors has been conducted in rat cardiac myocytes.<sup>6,12,14,15,20–22,26–28,30</sup> Therefore, the objectives of this study were to investigate the channels and the receptor pathways involved in the effect of noradrenaline on whole-cell  $I_{Kss}$  in atrial myocytes from the rat heart and to examine the contribution of  $I_{Kss}$  to changes in the atrial AP.

## 2. Methods

Further details are available in Supplementary material online.

### 2.1 Rat left atrial myocyte isolation

All animal procedures were approved by the ethics committee of the University of Bristol and performed in accordance with UK legislation [*Animals (Scientific Procedures) Act, 1986*]. Left atrial myocytes were isolated from adult male Wistar rats (200–320 g) as described previously.<sup>32</sup>

### 2.2 Whole-cell recording

Whole-cell currents and potentials were recorded using the whole-cell patch-clamp technique. Myocytes were superfused with Tyrode's solution comprising the following (in mM): 140 NaCl, 4 KCl, 1 MgCl<sub>2</sub>, 2.5 CaCl<sub>2</sub>, 10 D-glucose, and 5 HEPES, pH 7.4 at 36°C. For whole-cell, voltage-clamp current recording, the internal solution comprised the following (in mM): 10 NaCl, 110 KCl, 0.4 MgCl<sub>2</sub>, 5 D-glucose, 10 HEPES, 5 BAPTA, 5 K-ATP, and 0.5 Tris-GTP, pH 7.3 (KOH). Inward rectifier  $K^+$  currents were isolated using a voltage-ramp protocol and subtraction of the background current obtained in  $K^+$ -free external solution (see Supplementary material online, Figure S1). For  $K^+$ -free recordings, the external and internal solutions were created by equimolar replacement of KCl with CsCl. Iso-osmotic solution consisted of (in mM) 90 NaCl, 4 KCl, 1 MgCl<sub>2</sub>, 2.5 CaCl<sub>2</sub>, 10 D-glucose, 5 HEPES, and 100 Mannitol, pH 7.4 at 36°C (osmolality = 305 mOsm/kg H<sub>2</sub>O). Hypo-osmotic solution was produced by the omission

of mannitol (osmolality = 202 mOsm/kg H<sub>2</sub>O). Recordings for power spectral analysis were made in the presence of 10  $\mu$ M nifedipine. For current-clamp AP recording, the internal solution comprised the following (in mM): 10 NaCl, 110 KCl, 0.4 MgCl<sub>2</sub>, 5 D-glucose, 10 HEPES, 5 K-ATP, and 0.5 Tris-GTP, pH 7.3 (KOH). APs were elicited by 2 ms depolarizing current pulses at 1 Hz stimulation frequency.

### 2.3 PTX treatment of atrial myocytes

Atrial myocytes were incubated with PTX (1.5  $\mu$ g/mL) at 37°C for 3 h. Treatment with PTX under these conditions was sufficient to abolish the activation of  $I_{KACh}$  by 1  $\mu$ M ACh.

### 2.4 Drugs and reagents

All reagents were purchased from Sigma-Aldrich (Poole, UK), except PTX (Merck Chemicals Ltd, Nottingham, UK). Noradrenaline, fenoterol, atenolol, propranolol, ICI-118,551, zinc, fluoxetine, and mibefradil were dissolved in deionized water (dH<sub>2</sub>O) as 10 mM stock solutions and dissolved to the final concentration in the extracellular solution on the day of experiment. Prazosin was dissolved in near-absolute ethanol to make a 1 mM stock solution and dissolved to the final concentration in the extracellular solution on the day of experiment. Chromanol 293B, zinterol, and nifedipine were dissolved in dimethyl sulfoxide to make 10 mM stock solution of each drug and stored at –20°C. 4-AP was dissolved in dH<sub>2</sub>O to make 10 mM stock solution and the pH adjusted to 7.4 at 36°C with HCl. To avoid oxidation, 5,8,11,14-eicosatetraenoic acid (EYTA—a non-metabolizable arachidonic acid analogue) was dissolved in chloroform under a nitrogen atmosphere, and all chloroform evaporated before storage at –20°C. Stock solutions were diluted to the final concentration in the extracellular solution on the day of experiment. 1  $\mu$ M of the neurotransmitter was used as an effective concentration previously reported to inhibit  $I_{K1}$  and  $I_{Kss}$ .<sup>6,7</sup> The concentrations of prazosin (5  $\mu$ M), atenolol (10  $\mu$ M), ICI-118,551, and propranolol (1  $\mu$ M) used were chosen to achieve maximal effective blockade of, respectively,  $\alpha_{1-}$ ,  $\beta_{1-}$ ,  $\beta_{2-}$ , and combined  $\beta_{1-}/\beta_{2-}$  adrenoceptors.<sup>7,33–35</sup> Zinterol (1  $\mu$ M) and fenoterol (10  $\mu$ M) were used in the presence of 10  $\mu$ M atenolol to achieve selective  $\beta_{2-}$  adrenoceptor activation.<sup>34,35</sup> Protein kinase A (PKA) was inhibited using 10  $\mu$ M H-89, a concentration that has been shown to inhibit phosphorylation of the cardiac  $\alpha_{1c}$  L-type  $Ca^{2+}$  channel subunit.<sup>36</sup>

### 2.5 Data analysis

Current and voltage recordings were analysed using IgorPro (vs3.16B, Wavemetrics, Inc., USA). The voltage-dependence of the L-type  $Ca^{2+}$  current ( $I_{CaL}$ ) and the noradrenaline-sensitive steady-state outward current were fitted with modified Boltzmann equations. The variance of the noradrenaline-sensitive, steady-state outward current was calculated from the integral of the spectral density function, as described previously.<sup>14</sup>

### 2.6 Statistical analysis

Data are presented as the mean  $\pm$  SEM. Sample sizes are provided in the figure legends (numbers of cells/numbers of animals). Statistical analyses were performed using Prism (vs5.01, GraphPad Software, Inc., USA). Current–voltage relations were analysed by two-way repeated-measures (RM) analysis of variance (ANOVA) with the Bonferroni *post hoc* test. All other results were analysed by one-way ANOVA with Bonferroni's multiple comparisons test. A *P*-value of  $\leq 0.05$  was considered significant.

## 3. Results

### 3.1 Whole-cell currents modulated by noradrenaline

Two distinct current components were activated by square-shaped depolarizing pulses (500 ms) to potentials of –20 mV and positive:

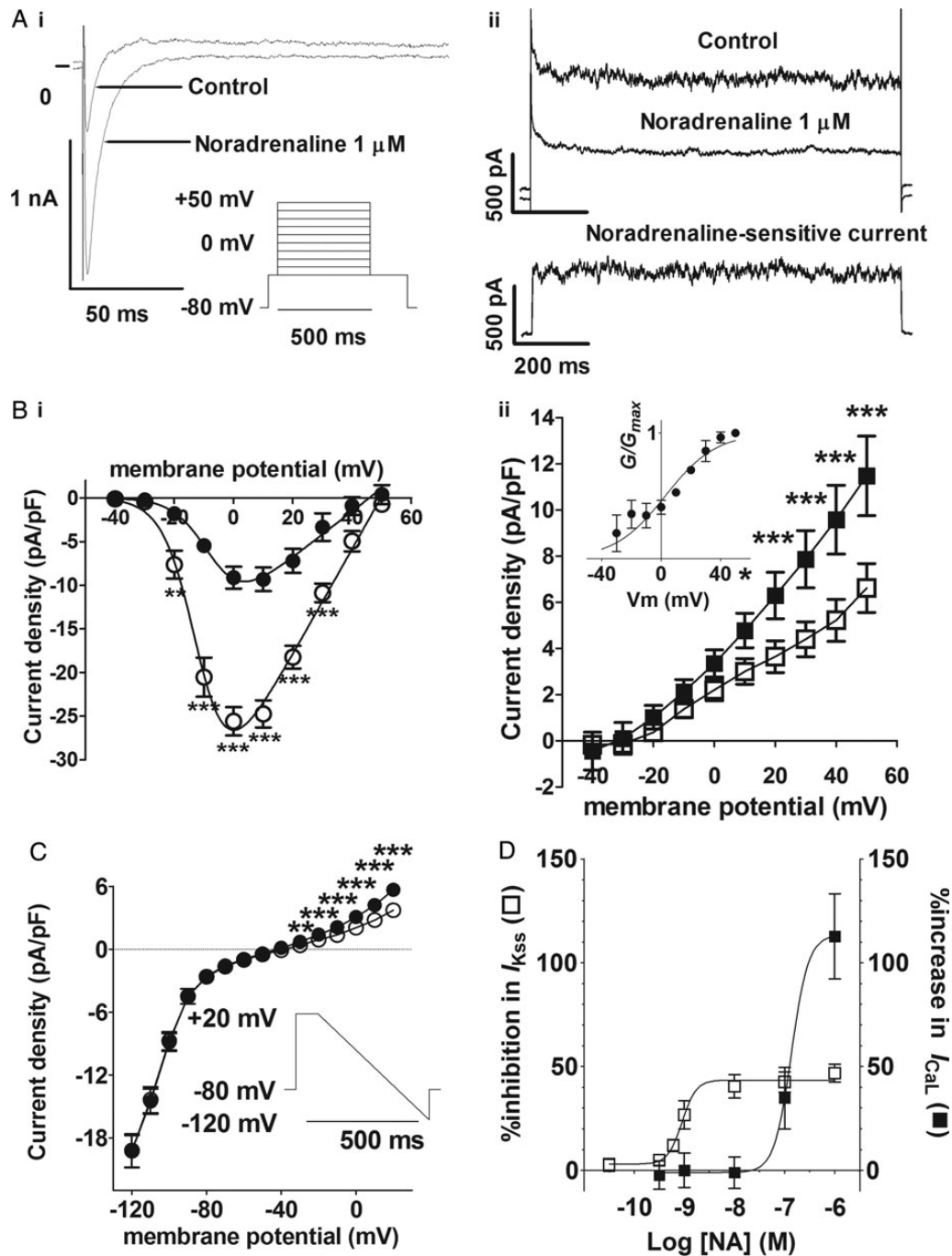


**Figure 1** Effects of noradrenaline on L-type  $\text{Ca}^{2+}$  ( $I_{CaL}$ ) and steady-state currents. (A) Example traces in control solution and in the presence of noradrenaline (1  $\mu\text{M}$ ) at 0 mV (i) and at +50 mV (ii). Inset in (i) shows the voltage protocol. Lower panel in (ii) shows the noradrenaline-sensitive current at +50 mV calculated as  $I_{\text{control}} - I_{\text{noradrenaline}}$  (scale bars, the same for upper and lower panels). (B) Mean current density–voltage relations from seven cells (five animals) for the peak inward current (i, circles) and the steady-state current (ii, squares). Control—filled symbols; 1  $\mu\text{M}$  noradrenaline—open symbols. Solid lines in (i) represent fits to a modified Boltzmann equation.  $G_{\text{max}}$ ,  $V_{\text{rev}}$ ,  $V_{\text{half}}$ , and  $k$  were, respectively, 0.265  $\text{kS F}^{-1}$ , +45.8 mV, -6.9 mV, and +5.8 mV in control and 0.603  $\text{kS F}^{-1}$ , +49.7 mV, -11.9 mV, and +5.5 mV in noradrenaline. Inset in (ii) shows the voltage-dependence of activation for the 1  $\mu\text{M}$  noradrenaline-sensitive difference current; solid line represents fit to a modified Boltzmann equation. (C) Effect of 1  $\mu\text{M}$  noradrenaline on mean background current–voltage relations ( $n = 6/2$ ). \* $P < 0.05$ ; \*\*\* $P < 0.001$ ; two-way RM ANOVA with the Bonferroni *post hoc* test. Inset shows a voltage-ramp protocol. (D) Concentration-dependent action of noradrenaline on the percentage inhibition of  $I_{Kss}$  (open squares) and percentage increase in  $I_{CaL}$  (filled squares) at +20 mV. Data from 4 to 16 cells/1–8 animals at each concentration. Solid lines represent a fit to a logistic equation.

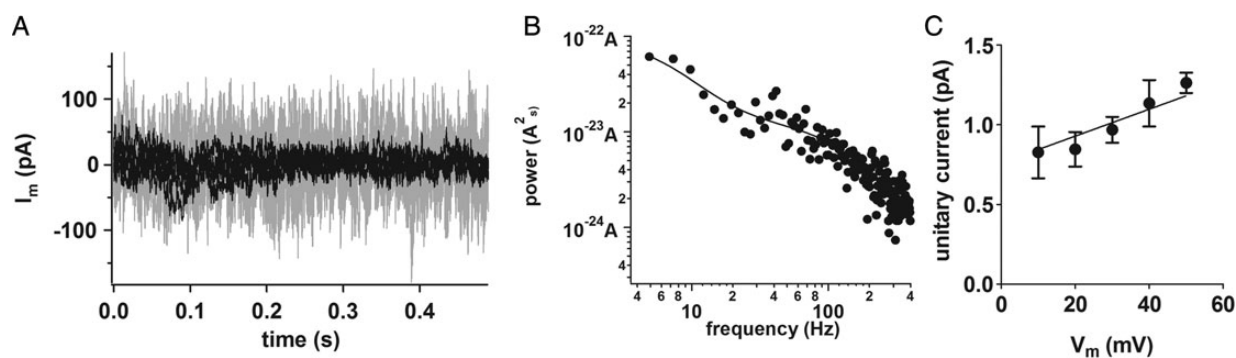


**Figure 2** Power spectral analysis of the noradrenaline-sensitive  $I_{K_{ss}}$ . (A) Five consecutive DC-subtracted traces recorded at +50 mV in control (grey traces) and in noradrenaline-containing (black traces) solution. (B) A representative power spectrum for the noradrenaline-sensitive current; data correspond to that shown in (A). Solid line represents a fit to a double Lorentzian equation;  $S(0)_1 = 8.15 \text{ pA}^2 \text{ s}^{-1}$ ,  $f_{c1} = 6.3 \text{ Hz}$ ,  $S(0)_2 = 1.15 \text{ pA}^2 \text{ s}^{-1}$ ,  $f_{c2} = 135.6 \text{ Hz}$ . (C) Mean unitary current–voltage relations for the noradrenaline-sensitive current ( $n = 8/6$ ). Solid line was fitted by linear regression assuming zero current at  $E_K$  ( $-90.9 \text{ mV}$ ).

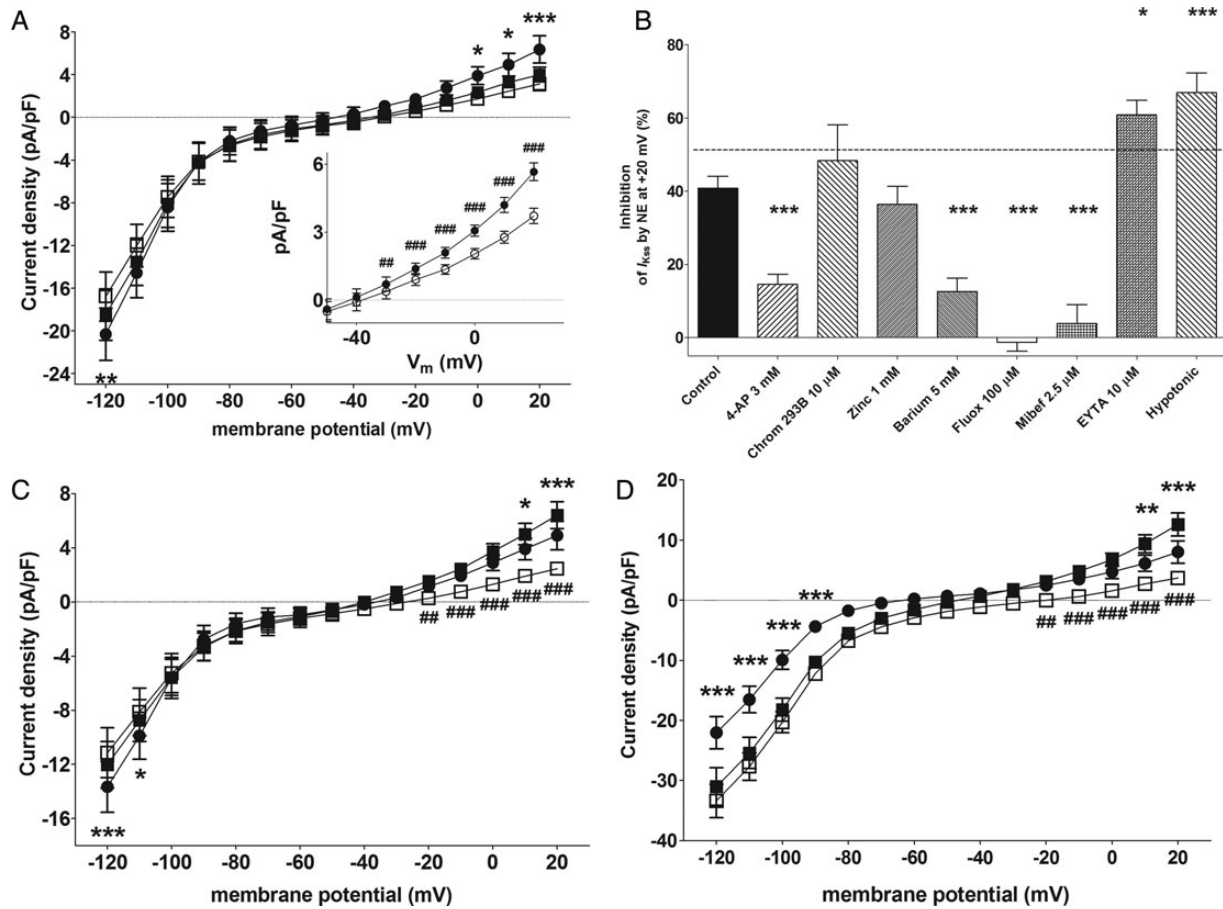
(i) an inward current that rapidly reached a peak and subsequently inactivated to a steady-state outward current level by the end of the pulse, representing the L-type  $\text{Ca}^{2+}$  current ( $I_{\text{CaL}}$ ) (Figure 1Ai) and (ii) a steady-state outward current that showed little inactivation at the end of the pulse (Figure 1Aii).  $I_{\text{CaL}}$  showed voltage-dependent activation with  $V_{\text{half}} \approx -7 \text{ mV}$  ( $k \approx 6 \text{ mV}$ ) and a maximal inward current density at 0 mV under control conditions (Figure 1Bi). Superfusion of the cells with  $1 \mu\text{M}$  noradrenaline produced a marked increase in  $I_{\text{CaL}}$  across the voltage range, and this was associated with a  $\sim 2.3$ -fold increase in  $G_{\text{max}}$  and a  $\sim 5 \text{ mV}$  negative shift in  $V_{\text{half}}$ . In addition,  $1 \mu\text{M}$  noradrenaline also inhibited the steady-state outward current at positive potentials, the current at +50 mV being reduced by  $42.1 \pm 4.3\%$  ( $n = 7/5$ ) (Figure 1Bii). Note the time-independent nature of the noradrenaline-sensitive outward current at +50 mV (lower panel, Figure 1Aii). The noradrenaline-sensitive outward current component was weakly voltage-dependent ( $V_{\text{half}} = 2.71 \pm 3.22 \text{ mV}$ ,  $k = 17.11 \pm 3.04 \text{ mV}$ ), being activated from potentials positive to  $-40 \text{ mV}$  (inset, Figure 1Bii). The inwardly rectifying current obtained at negative potentials using a modified ramp protocol was abolished in the absence of external  $\text{K}^+$  (see Supplementary material online, Figure S1), demonstrating the involvement of  $\text{K}_{\text{ir},2.x}$  channels.<sup>37</sup> While  $1 \mu\text{M}$  noradrenaline inhibited the steady-state outward currents evident at potentials positive to  $-40 \text{ mV}$  (Figure 1Bii), the currents negative to  $-40 \text{ mV}$  were unaffected (Figure 1C). Thus, under the conditions of this study, noradrenaline inhibited a time-independent, outwardly rectifying weakly voltage-dependent current, whereas  $I_{K1}$  was unaffected (see Supplementary material online, Figure S1E). Noradrenaline ( $1 \mu\text{M}$ ) had similar effects on whole-cell currents in isolated mouse atrial myocytes (see Supplementary material online, Figure S2). The effects of noradrenaline on the steady-state outward current were abolished in the absence of internal and external  $\text{K}^+$ , demonstrating the  $\text{K}^+$ -selective nature of the noradrenaline-sensitive  $I_{K_{ss}}$  (see Supplementary material online, Figure S3B). In rat atrial cells,  $I_{K_{ss}}$  was inhibited concentration-dependently by noradrenaline with  $\log(\text{IC}_{50}) = -9.048 \pm 0.0979 \text{ M}$  ( $\text{EC}_{50} = 0.895 \text{ nM}$ ), whereas  $I_{\text{CaL}}$  was potentiated with a  $\log(\text{EC}_{50}) = -6.687 \pm 2.882 \text{ M}$  ( $\text{EC}_{50} = 136 \text{ nM}$ ) (Figure 1D). Thus, noradrenaline was  $\sim 150$ -fold more potent in the inhibition of  $I_{K_{ss}}$  than in the increase of  $I_{\text{CaL}}$ .

### 3.2 Power spectral analysis of noradrenaline-sensitive $I_{K_{ss}}$

It was notable in the recordings of steady-state outward currents in the presence of  $\text{K}^+$  that the level of noise in  $I_{K_{ss}}$  was reduced by noradrenaline (Figure 1Aii). This is demonstrated in Figure 2A, in which 5 DC-component-subtracted currents at +50 mV in the presence of noradrenaline (black traces) are superimposed on 5 DC-subtracted control currents (grey). This reduction in noise reflects the action of noradrenaline on the gating of the underlying  $\text{K}^+$ -selective channels. Because the open-channel conductance is a function of the current variance, the power spectra provide a measure of the unitary conductance.<sup>38</sup> The power spectra could be described by a double Lorentzian (Figure 2B), in which the corner frequencies (mean values at +50 mV in parentheses),  $f_{c1}$  ( $4.1 \pm 1.6 \text{ Hz}$ ) and  $f_{c2}$  ( $148.5 \pm 25.3 \text{ Hz}$ ), are functions of channel gating and the low-frequency asymptotes;  $S(0)_1$  ( $572 \pm 251 \text{ pA}^2 \text{ s}^{-1}$ ) and  $S(0)_2$  ( $4.70 \pm 1.04 \text{ pA}^2 \text{ s}^{-1}$ ) are functions of the power of the noise arising from channel gating ( $n = 8/6$  cells). The open-channel conductance calculated by a linear regression of the unitary current–voltage relations was  $8.44 \pm 0.42 \text{ pS}$  (Figure 2C,  $n = 8/6$ ).

### 3.3 Sensitivity of $I_{K_{ss}}$ to $\text{K}^+$ channel modulators

The outward currents at positive potentials were reduced by the blocker of voltage-gated  $\text{K}^+$  channels, 4-AP ( $3 \text{ mM}$ ),<sup>39</sup> although noradrenaline in the continued presence of 4-AP inhibited the current further so that the response to noradrenaline at +20 mV was reduced to  $\sim 36\%$  of control (Figure 3A and B). On the other hand, neither the  $\text{KCNQ1}/I_{K_s}$  delayed rectifier channel blocker, chromanol 293B ( $10 \mu\text{M}$ ),<sup>40</sup> nor the TASK-1/TASK-3 blocker,  $\text{Zn}^{2+}$  ( $1 \text{ mM}$ ),<sup>41,42</sup> had any significant effect on the response to noradrenaline, although the control steady-state outward current was reduced by  $28.9 \pm 4.1\%$  ( $n = 5/2$ ) in the presence of the divalent cation (Figure 3B). These data are consistent with the proposition that TASK-1/3 contributes to an outward current in rat atrial myocytes that is not modulated by noradrenaline. On the other hand, the background currents at both positive and negative potentials were markedly inhibited by the TREK-1 blockers, fluoxetine and mibefradil (see Supplementary material online,



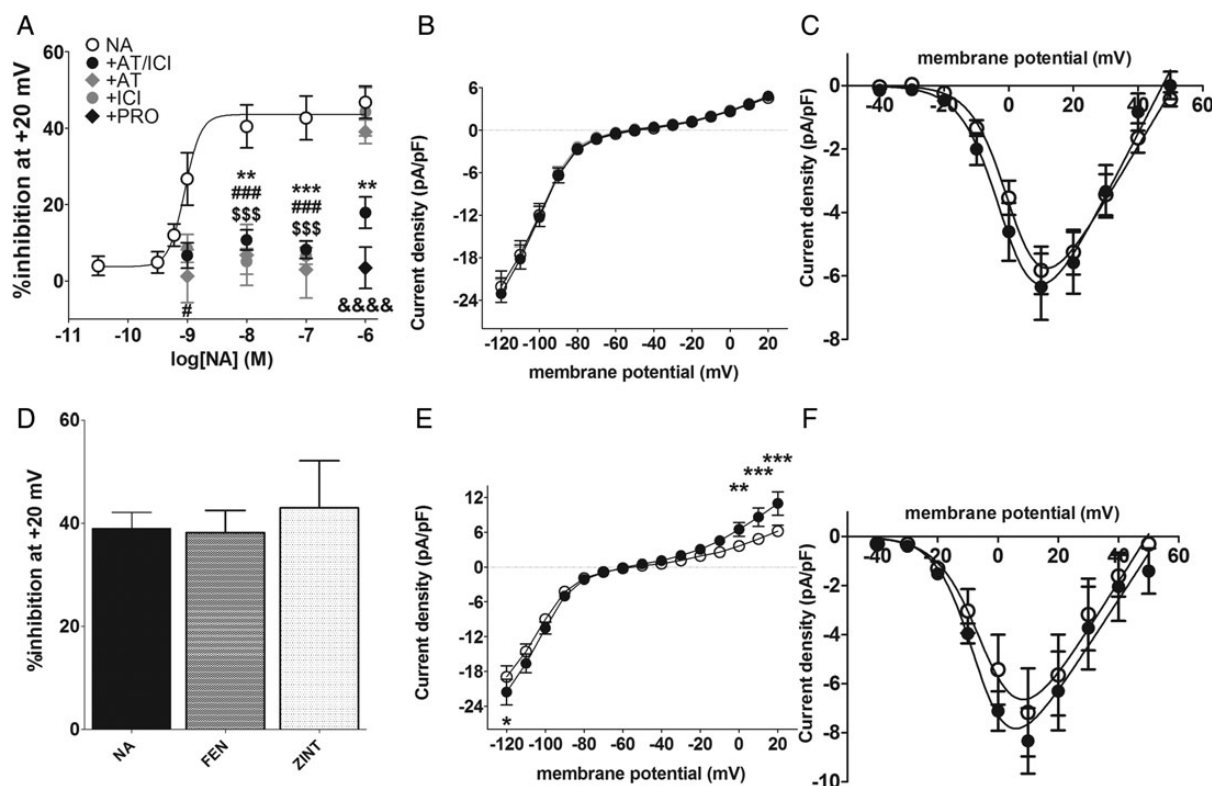
**Figure 3** Effect of  $K^+$  channel modulators on the noradrenaline-sensitive current. (A) Mean background current density–voltage relations from six cells/two animals in control solution (filled circles), in the presence of 4-AP (3 mM, filled squares) and in the presence of 4-AP + noradrenaline (1  $\mu$ M, open squares). Inset reproduces the effect of noradrenaline under control conditions shown in Figure 1D over the voltage range,  $-50$  to  $+20$  mV. 4-AP vs. control: \* $P < 0.05$ ; \*\* $P < 0.01$ ; \*\*\* $P < 0.001$ ; inset noradrenaline vs. control: ## $P < 0.01$ ; ### $P < 0.001$ ; two-way RM ANOVA with the Bonferroni *post hoc* test. (B) Effect of  $K^+$  channel modulators on the mean percentage inhibition by noradrenaline of  $I_{KSS}$  at  $+20$  mV. Control ( $n = 8/6$ ), 4-AP ( $n = 6/2$ ), chromanol 293 B (Chrom 293B;  $n = 5/1$ ),  $Zn^{2+}$  ( $n = 5/2$ ),  $Ba^{2+}$  ( $n = 7/1$ ), fluoxetine (fluox;  $n = 7/2$ ), mibefradil (mibef;  $n = 6/2$ ), EYTA ( $n = 5/3$ ), and hypotonic solution ( $n = 7/2$ ). \*\* $P < 0.01$ ; \*\*\* $P < 0.001$ ; one-way ANOVA with the Bonferroni multiple comparisons test vs. control. (C) Mean background current density–voltage relations in control solution (filled circles) and in the presence of EYTA (1  $\mu$ M, filled squares) and in the presence of EYTA + noradrenaline (1  $\mu$ M, open squares,  $n = 5/3$ ). \* $P < 0.05$ ; \*\*\* $P < 0.001$ ; two-way RM ANOVA with the Bonferroni *post hoc* test, EYTA vs. control. ## $P < 0.01$ ; ### $P < 0.001$ ; two-way RM ANOVA with the Bonferroni *post hoc* test, noradrenaline + EYTA vs. EYTA. (D) Mean background current density–voltage relations in control solution (filled circles), in the presence of hypotonic solution (filled squares) and in the presence of hypotonic solution + noradrenaline (1  $\mu$ M, open squares,  $n = 7/2$ ). \*\* $P < 0.01$ ; \*\*\* $P < 0.001$ ; two-way RM ANOVA with the Bonferroni *post hoc* test, hypotonic vs. control. ## $P < 0.01$ ; ### $P < 0.001$ ; two-way RM ANOVA with the Bonferroni *post hoc* test, noradrenaline + hypotonic vs. hypotonic.

Figure S4).<sup>43–46</sup> The fluoxetine- and mibefradil-sensitive difference currents reversed close to the  $K^+$  equilibrium potential ( $E_K$ ), demonstrating their  $K^+$ -selectivity (see Supplementary material online, Figure S4B and D). Most strikingly, the effect of noradrenaline on the steady-state outward current was abolished in the presence of the TREK-1 channel blockers (Figure 3B). TREK-1 channel currents are reported to be activated by arachidonic acid and by stretch.<sup>20–22,24,47</sup> The effect of the non-metabolizable analogue of arachidonic acid, EYTA (10  $\mu$ M), on the noradrenaline-sensitive current was investigated (Figure 3C). Superfusion of the cells with EYTA increased the steady-state outward current at  $+20$  mV by  $38.6 \pm 16.2\%$  ( $P < 0.05$ ;  $n = 5/3$ ; Figure 3C). Addition of noradrenaline in the continued presence of EYTA resulted in a reduction of the steady-state outward current by  $60.9 \pm 3.9\%$  ( $P < 0.001$ ;  $n = 5/3$ ; Figure 3C), representing an augmentation of the

response to noradrenaline of  $\sim 50\%$  (Figure 3B). Similarly, hypotonic stretch also increased  $I_{KSS}$  at  $+20$  mV ( $69.7 \pm 17.0\%$ ,  $n = 7/2$ ,  $P < 0.05$ ), and noradrenaline inhibited the hypototically potentiated current ( $67.0 \pm 12.6\%$ ;  $P < 0.001$ ), representing  $\sim 63\%$  augmentation of the response to noradrenaline (Figure 3B and D).

### 3.4 Adrenoceptor subtypes in the noradrenaline response

The inhibitory effect of noradrenaline on  $I_{KSS}$  at concentrations of 1–100 nM was strongly reduced by either the  $\beta_1$ -adrenoceptor blocker, atenolol (10  $\mu$ M), or  $\beta_2$ -selective ICI-118,551 (100 nM; Figure 4A). However, neither antagonist was effective against the response to 1  $\mu$ M noradrenaline when applied alone (Figure 4A). On the



**Figure 4** Effect of adrenoceptor antagonists on the effects of noradrenaline. (A) Effect of adrenoceptor antagonists on the concentration-dependence of mean percentage  $I_{K_{SS}}$  inhibition by noradrenaline at +20 mV. Control (open circles,  $n = 8/6$ ), atenolol (grey-filled diamonds,  $n = 11/4$ ), ICI-118,551 (grey-filled circles,  $n = 10/4$ ), atenolol plus ICI-118,551 (black-filled circles,  $n = 5/2$ ), and propranolol (black-filled diamonds,  $n = 8/4$ ). Solid line represents a fit to a logistic equation. Control data as shown in Figure 1D.  $\#P < 0.05$  and  $\#\#\#P < 0.001$ ; two-way ANOVA with the Bonferroni *post hoc* test, atenolol vs. control.  $\$\$\$P < 0.001$ , two-way ANOVA with the Bonferroni *post hoc* test, ICI-118,551 vs. control.  $\ast\ast P < 0.01$  and  $\ast\ast\ast P < 0.001$ ; two-way ANOVA with the Bonferroni *post hoc* test, atenolol/ICI-118,551 vs. control.  $\&\&\&P < 0.0001$ , Student's paired *t*-test, propranolol vs. control. (B) Mean background current–voltage relations in control (grey-filled circles), in the presence of 1  $\mu\text{M}$  propranolol (black-filled circles) and in the presence of propranolol + noradrenaline (open circles,  $n = 8/4$ ). Note that the IV curves are almost completely superimposed. (C) Mean  $I_{CaL}$  density–voltage relations in the presence of propranolol (filled circles) and in the presence of propranolol + noradrenaline (open circles,  $n = 9/4$ ).  $I_{CaL}$ –V relation in the presence of propranolol alone was not significantly different from control (Figure 1Bi,  $P = 0.1388$ , two-way ANOVA with RM for voltage). (D) Mean percentage inhibition of  $I_{K_{SS}}$  at +20 mV by  $\beta_2$ -agonists, noradrenaline (1  $\mu\text{M}$ ,  $n = 11/4$ ), fenoterol (10  $\mu\text{M}$ ,  $n = 8/3$ ), and zinterol (1  $\mu\text{M}$ ,  $n = 6/2$ ) in the presence of 10  $\mu\text{M}$  atenolol. (E) Effect of 1  $\mu\text{M}$  zinterol on mean background current density–voltage relations in the presence of 10  $\mu\text{M}$  atenolol ( $n = 6/2$ ). Filled circles—control; open circles—1  $\mu\text{M}$  zinterol.  $\ast P < 0.05$ ;  $\ast\ast P < 0.01$ ;  $\ast\ast\ast P < 0.001$ ; two-way ANOVA with the Bonferroni *post hoc* test, zinterol vs. control at each voltage. (F) Effect of 1  $\mu\text{M}$  zinterol on  $I_{CaL}$  density–voltage relations in the presence of 10  $\mu\text{M}$  atenolol ( $n = 5/2$ ). Solid lines in (C and F) represent fits to modified Boltzmann equations.

other hand, the effect of 1  $\mu\text{M}$  noradrenaline was markedly inhibited when the  $\beta_1$ - and  $\beta_2$ -antagonists, atenolol (10  $\mu\text{M}$ ) and ICI-118,551 (100 nM), were applied in combination (Figure 4A). The apparent rightward-shift in the concentration-dependence of  $I_{K_{SS}}$  inhibition by noradrenaline produced by either atenolol or ICI-118,551 when applied alone, taken together with the cumulative effect against 1  $\mu\text{M}$  noradrenaline when the antagonists were applied in combination, demonstrates the involvement of both  $\beta_1$ - and  $\beta_2$ -adrenoceptor subtypes in response to noradrenaline. Consistent with this, the effect of 1  $\mu\text{M}$  noradrenaline on  $I_{K_{SS}}$  was abolished by the non-selective  $\beta_1/\beta_2$ -adrenoceptor antagonist, propranolol (1  $\mu\text{M}$ ; Figure 4A and B). The effect of 1  $\mu\text{M}$  noradrenaline on the steady-state outward current at +20 mV ( $46.8 \pm 2.56\%$ ,  $n = 13$ ) was unaffected by the  $\alpha$ -adrenoceptor antagonist, prazosin (5  $\mu\text{M}$ ), either applied alone ( $46.6 \pm 4.06\%$ ,  $n = 5$ ) or in combination with 10  $\mu\text{M}$  atenolol ( $42.3 \pm 5.11\%$ ,  $n = 5$ ).  $I_{K_{SS}}$  was inhibited by  $\beta_2$ -adrenoceptor-selective agonism with either zinterol

(1  $\mu\text{M}$ ) or fenoterol (10  $\mu\text{M}$ ) in the presence of 10  $\mu\text{M}$  atenolol, in a manner similar to noradrenaline, consistent with a role for  $\beta_2$ -adrenoceptors in the inhibition of  $I_{K_{SS}}$  (Figure 4D and E). The augmentation of  $I_{CaL}$  by 1  $\mu\text{M}$  noradrenaline was also completely inhibited in the presence of propranolol (Figure 4C). The increase of  $I_{CaL}$  by 1  $\mu\text{M}$  noradrenaline ( $201 \pm 54.6\%$  at +10 mV,  $n = 6$ , Figure 1Bi) was also completely abolished in the presence of the  $\beta_1$ -adrenoceptor antagonist, 10  $\mu\text{M}$  atenolol ( $-3.1 \pm 2.69\%$ ,  $n = 5$ ). On the other hand, zinterol had no effect on  $I_{CaL}$  (Figure 4F), indicating that the effect of noradrenaline on  $I_{CaL}$  was mediated predominantly by  $\beta_1$ -adrenoceptors.

### 3.5 Cell signalling pathways

The  $\beta_2$ -adrenoceptor couples with both  $G_s$ - and  $G_i$ -mediated signalling pathways.<sup>3</sup>  $G_s$ -protein activates the adenylyl cyclase/PKA cascade involving cyclic AMP.<sup>3</sup> The inhibitory effect of noradrenaline on the steady-state outward current could still be observed following

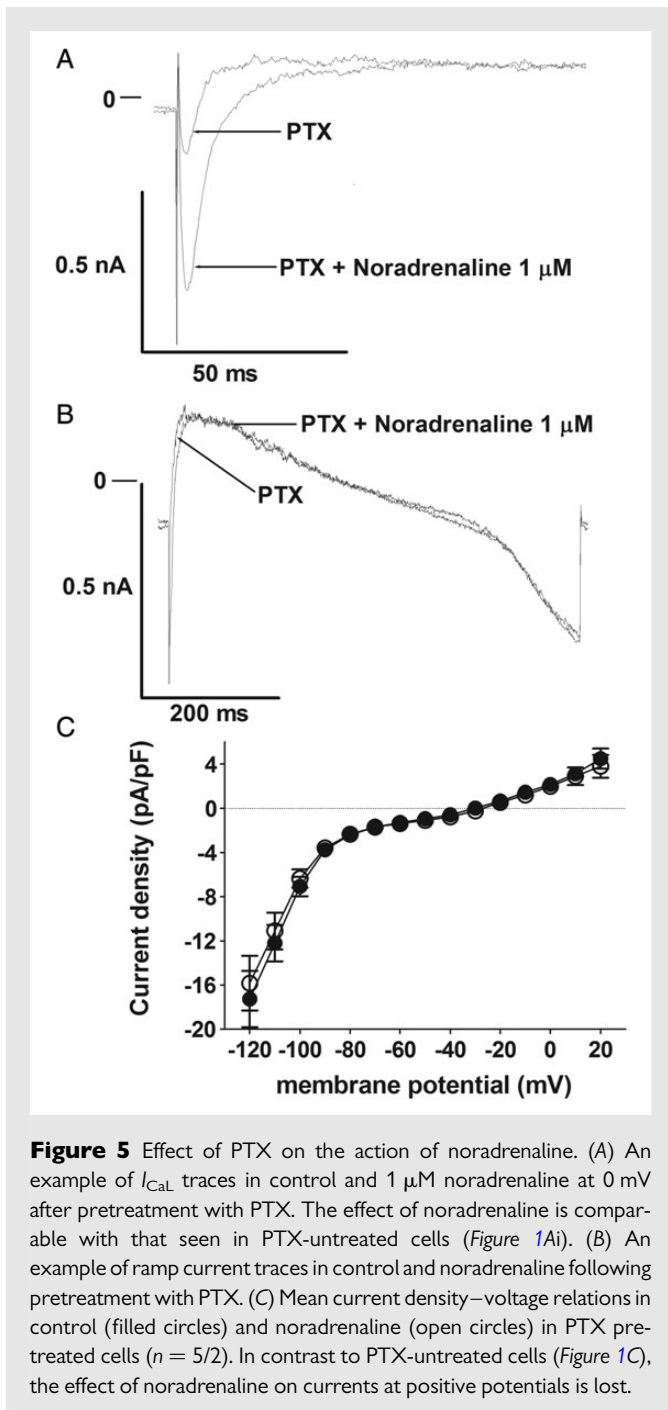


**Figure 5** Effect of PTX on the action of noradrenaline. (A) An example of  $I_{CaL}$  traces in control and 1  $\mu$ M noradrenaline at 0 mV after pretreatment with PTX. The effect of noradrenaline is comparable with that seen in PTX-untreated cells (Figure 1Ai). (B) An example of ramp current traces in control and noradrenaline following pretreatment with PTX. (C) Mean current density–voltage relations in control (filled circles) and noradrenaline (open circles) in PTX pretreated cells ( $n = 5/2$ ). In contrast to PTX-untreated cells (Figure 1C), the effect of noradrenaline on currents at positive potentials is lost.

treatment of the cells with the PKA inhibitor, H-89 (10  $\mu$ M), at a concentration sufficient to ablate completely the augmentation of  $I_{CaL}$  (see Supplementary material online, Figure S5), indicating that PKA was not essential to the action of noradrenaline on  $I_{Kss}$ . The role of  $G_i$ -proteins in the inhibitory effect of noradrenaline on the steady-state outward current was investigated by pretreatment of the cells in PTX (Figure 5). While the effect of noradrenaline on  $I_{CaL}$  remained intact in PTX-treated cells (Figure 5A), the steady-state outward current inhibition was completely abolished (Figure 5B and C). Taken together, these results show that the inhibitory effect of noradrenaline on the steady-state outward current was mediated via a PTX-sensitive mechanism that did not require PKA. On the other hand,  $\beta_2$ -adrenoceptors did not contribute

to the potentiation of  $I_{CaL}$  by noradrenaline, which likely involved  $\beta_1$ -adrenoceptors acting via PKA.

### 3.6 AP prolongation by noradrenaline

The effects of noradrenaline (1  $\mu$ M) on the AP were investigated (Figure 6). Noradrenaline caused a delay in the early and mid-phases of repolarization, consistent with changes in  $I_{CaL}$  and  $I_{Kss}$  (Figure 6A). The effect of noradrenaline in the presence of the  $\beta_1$ -antagonist, atenolol, and the non-selective  $\beta_1/\beta_2$ -blocker, propranolol, is shown in Figure 6B and C, respectively. The effects of noradrenaline on mean AP duration at 30% repolarization ( $APD_{30}$ ) in the absence of and the presence of the  $\beta$ -blockers are shown in Figure 6D. Noradrenaline caused  $\sim 65\%$  prolongation of  $APD_{30}$ . Although  $\beta_1$ -antagonism produced a partial reduction in  $APD_{30}$  prolongation, the effect of noradrenaline was completely abolished with combined  $\beta_1/\beta_2$ -blockade using either 100 nM ICI-118,551 in combination with 10  $\mu$ M atenolol or 1  $\mu$ M propranolol (Figure 6D).

## 4. Discussion

This study demonstrates for the first time the potent inhibition of a steady-state outward  $K^+$  current in atrial myocytes by nanomolar concentrations of noradrenaline ( $IC_{50} = 0.90$  nM). In contrast, noradrenaline was  $\sim 150$ -fold less potent in potentiating  $I_{CaL}$  ( $EC_{50} = 136$  nM). Both  $\beta_1$ - and  $\beta_2$ -adrenoceptors were co-operatively involved in the inhibition of  $I_{Kss}$ , which was via a PTX-sensitive pathway that did not require PKA. On the other hand, the potentiation of  $I_{CaL}$  by noradrenaline was mediated via  $\beta_1$ -adrenoceptors through PKA. The noradrenaline-sensitive current had pharmacological and biophysical properties consistent with the involvement of a TREK-like channel. Inhibition of  $I_{Kss}$  contributed to the noradrenaline-induced prolongation of the AP in atrial myocytes.

### 4.1 Properties of noradrenaline-sensitive

#### $I_{Kss}$

The effectively instantaneous activation of the noradrenaline-sensitive steady-state outward current on depolarization positive to  $-40$  mV and the lack of time-dependent inactivation over the course of the pulse are representative of adrenoceptor-modulated  $I_{Kss}$  in rat ventricular myocytes reported previously and rule out contribution of the transient outward current,  $I_{to}$ .<sup>6,12,14</sup> Moreover, the observation that 36% of the noradrenaline-sensitive current remained in the presence of 3 mM 4-AP indicates that  $I_{Kss}$  was distinct from the comparatively 4-AP-sensitive  $I_{Kur}/K_v1.5$  channel currents that would be almost completely inhibited by the concentration of this voltage-gated  $K^+$  channel blocker.<sup>15,19</sup>

Although control  $I_{Kss}$  was inhibited by  $Zn^{2+}$ , consistent with the contribution of TASK-1 channels to the whole-cell currents, the response to noradrenaline was unaffected, demonstrating that this  $K_{2P}$  channel did not contribute to the noradrenaline-sensitive current. On the other hand, the weak voltage-dependence, the potentiation by the arachidonic acid analogue, EYTA, and by osmotic stretch and the inhibition by fluoxetine, mibefradil, and  $Ba^{2+}$  are all properties that noradrenaline-sensitive  $I_{Kss}$  shares with TREK-1 channels.<sup>20–22,43–47</sup> The effects of noradrenaline on the power spectrum demonstrate unequivocally the involvement of an ion channel with flickery kinetics in  $I_{Kss}$ . The calculated unitary conductance (8.4 pS) is close to the 14 pS originally proposed for TREK-1.<sup>48</sup> However, unitary current recordings of TREK-1-like

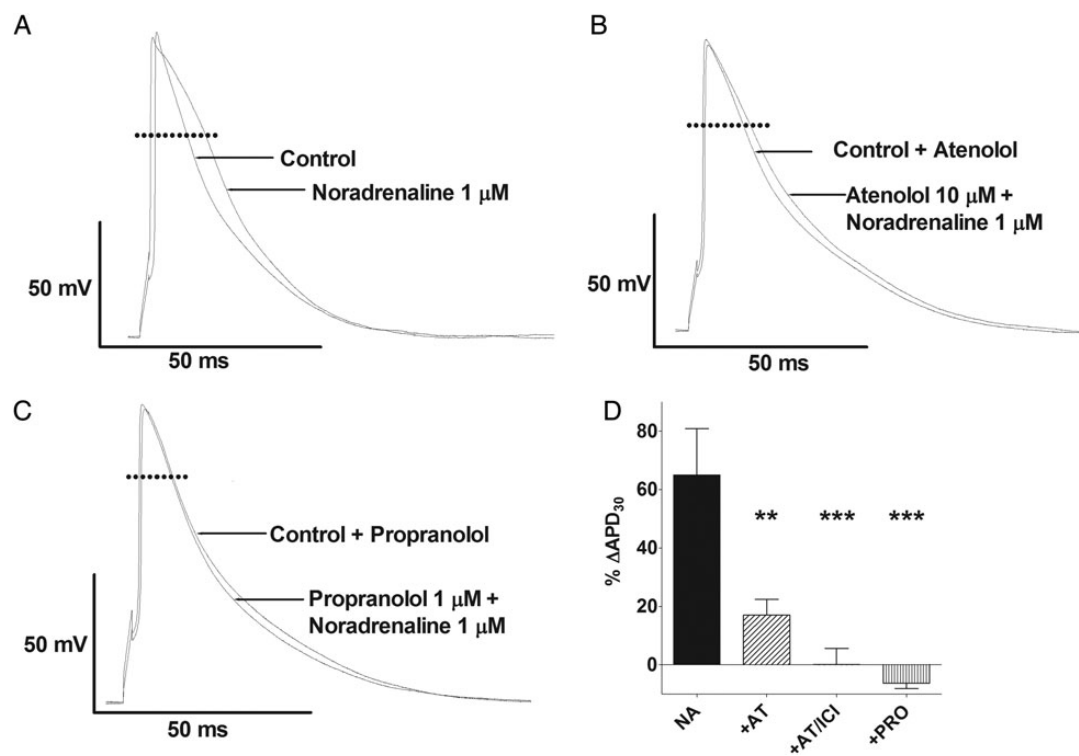


**Figure 6** Effects of noradrenaline on APs. (A) Representative APs in control and in 1  $\mu$ M noradrenaline. (B) Representative APs in the presence of 10  $\mu$ M atenolol and 1  $\mu$ M noradrenaline in the continued presence of atenolol. (C) Representative APs in the presence of 1  $\mu$ M propranolol and 1  $\mu$ M noradrenaline in the continued presence of propranolol. (D) Mean noradrenaline-induced percentage APD<sub>30</sub>-change (% $\Delta$ APD<sub>30</sub>) in the absence of antagonist (NA,  $n = 5/4$ ), in the presence of 10  $\mu$ M atenolol (+AT,  $n = 8/4$ ), in the presence of 100 nM ICI-118,551 plus 10  $\mu$ M atenolol (+AT/ICI,  $n = 6/2$ ), and in the presence of 1  $\mu$ M propranolol (+PRO,  $n = 5/2$ ). \*\* $P < 0.01$ ; \*\*\* $P < 0.001$ ; one-way ANOVA with the Bonferroni *post hoc* test.

channel currents in rat cardiomyocytes have suggested a conductance of  $\sim 41$  pS.<sup>21,22</sup> The basis for the differences in reported conductance are unclear, but a number of conductance modes for the TREK-1 channel have been reported, and it has been suggested that the conductance mode depends on interaction with cytosolic regulatory proteins.<sup>49</sup> It is conceivable, therefore, that the noradrenaline-sensitive channel represents a lower conductance mode of TREK-1 than was evident previously in cell-attached and excised-patch recordings.<sup>21,22</sup> It is notable that  $I_{K_{SS}}$  was also reduced by the removal of external  $K^+$  in a manner reminiscent of  $K_{ir}$  channels. Nevertheless,  $I_{K_{SS}}$  was distinct from  $I_{K1}$ , because noradrenaline had no effect on the inward rectifier currents. Interestingly, a tendency to pore collapse and non-conductive states of the channel in external  $K^+$ -free conditions similar to  $K_{ir,2.1}$  has recently been suggested for TREK-1.<sup>50</sup> Thus, our data are consistent with the involvement of a TREK-1-like channel in the noradrenaline-sensitive  $I_{K_{SS}}$  of rat atrial myocytes.

#### 4.2 Inhibition of $I_{K_{SS}}$ is mediated via a PTX-sensitive mechanism involving both $\beta_1$ - and $\beta_2$ -adrenoceptors

The effect of receptor subtype-selective concentrations of atenolol (10  $\mu$ M) and ICI-118,551 (100 nM)<sup>33–35</sup> on the concentration response of  $I_{K_{SS}}$  inhibition by noradrenaline demonstrated the involvement of both  $\beta_1$ - and  $\beta_2$ -adrenoceptors. Either atenolol or ICI-118,551 was effective at inhibiting responses to 1–100 nM noradrenaline,

indicating co-operativity between  $\beta_1$ - and  $\beta_2$ -adrenoceptor pathways. It is notable that noradrenaline was effective at inhibiting  $I_{K_{SS}}$  at concentrations far below the reported dissociation constant at either  $\beta_1$ - ( $K_d \sim 1–4$   $\mu$ M) or  $\beta_2$ -adrenoceptors ( $K_d \sim 4–26$   $\mu$ M).<sup>51–53</sup> Interestingly, it has been reported that  $\beta_1$ -/ $\beta_2$ -adrenoceptor subunits can form heterodimeric receptors in cardiomyocytes that have an increased agonist sensitivity relative to the respective homodimeric receptors.<sup>54</sup> Moreover, the action of noradrenaline in inhibiting  $I_{K_{SS}}$  with greater potency than potentiation of  $I_{CaL}$  is consistent with a previous report of the effects of the  $\beta$ -agonist, isoprenaline, on  $I_{K_{SS}}$  and  $I_{CaL}$  in rat ventricular myocytes.<sup>12</sup>

The abolition of  $I_{K_{SS}}$  responses following pretreatment with PTX demonstrated the involvement of a  $G_i$ -protein, consistent with reports of coupling of  $\beta_1$ -, as well as  $\beta_2$ -adrenoceptors, to  $G_i$ -protein pathways in cardiomyocytes.<sup>55,56</sup> The involvement of  $\beta$ -adrenoceptors in the inhibition of TREK-1 channel-like currents in rat atrial myocytes has been suggested previously.<sup>21</sup> However, the inhibitory response to noradrenaline was not abolished by treatment with H-89, indicating that PKA was not required for the regulation of  $I_{K_{SS}}$ . Although the effect of noradrenaline on  $I_{K_{SS}}$  was reduced in the presence of H-89, this was likely due to non-specific actions of the PKA inhibitor.<sup>57</sup> The requirement of both  $\beta_1$ - and  $\beta_2$ -adrenoceptors for  $I_{K_{SS}}$  inhibition by noradrenaline and the PTX sensitivity of this response suggest that the receptors and  $G_i$ -proteins modulating TREK-like channel activity are co-localized, consistent with the ability of  $\beta_1$ -/ $\beta_2$ -adrenoceptor subtypes to form heterodimers.<sup>54</sup>



The potentiation of  $I_{CaL}$  by noradrenaline was mediated predominantly via a PTX-insensitive, H-89-sensitive  $\beta_1$ -adrenoceptor pathway, consistent with an essential role for PKA in the regulation of cardiac L-type  $Ca^{2+}$  channels.<sup>56,58</sup>  $I_{CaL}$  was not potentiated by zinterol, indicating that, in contrast to ventricular cells,  $\beta_2$ -adrenoceptors were not involved in the regulation of L-type  $Ca^{2+}$  channels in rat atrial myocytes.<sup>56,59</sup> Consistent with this view, the potentiation of  $I_{CaL}$  by 1  $\mu$ M noradrenaline was completely abolished in the presence of  $\beta_1$ -receptor-selective atenolol.

### 4.3 Noradrenergic inhibition of $I_{Kss}$ contributes to AP prolongation

Noradrenaline caused prolongation of the AP at relatively depolarized potentials, but had little effect closer to the resting membrane potential. The prolongation of APD<sub>30</sub> by noradrenaline was consistent with the actions of noradrenaline on  $I_{CaL}$  and  $I_{Kss}$ . Under the conditions of this study, it was possible to discriminate between the actions of noradrenaline on  $I_{CaL}$  and  $I_{Kss}$  through differences in their sensitivity to  $\beta$ -adrenoceptor-selective antagonists. For example, in the presence of atenolol alone, noradrenergic potentiation of  $I_{CaL}$  would be blocked while the inhibition of  $I_{Kss}$  would remain intact. On the other hand, in the presence of combined  $\beta_1$ -/ $\beta_2$ -antagonism, the effect of noradrenaline on  $I_{Kss}$  would also be reduced. Thus, the correlation between the degree of noradrenaline-induced APD<sub>30</sub> prolongation and the degree of noradrenergic inhibition of  $I_{Kss}$  in the presence of  $\beta_1$ -/ $\beta_2$ -non-selective propranolol,  $\beta_1$ -selective atenolol, and  $\beta_2$ -selective ICI-118,551 in combination and atenolol alone (see Supplementary material online, Figure S6) illustrated the contribution of  $I_{Kss}$  to the noradrenergic prolongation of the AP. AP prolongation through  $I_{Kss}$  inhibition is likely to affect sarcolemmal  $Ca^{2+}$  fluxes via L-type  $Ca^{2+}$  channels and the  $Na^+$ / $Ca^{2+}$  exchanger and thereby to contribute to the effects of noradrenaline on atrial contractility and arrhythmogenesis.

### 4.4 Possible physiological significance of noradrenaline-sensitive $I_{Kss}$

It has not been possible, to date, to measure directly the concentration of noradrenaline achieved at the neuroeffector junction of cardiac post-ganglionic fibres during sympathetic activity, but it is generally estimated to be >100 nM.<sup>60</sup> The EC<sub>50</sub> for noradrenergic potentiation of  $I_{CaL}$  corresponds well with this value, consistent with the potentiation via  $\beta_1$ -adrenoceptors of atrial  $Ca^{2+}$  entry during sympathetic activity.<sup>2,4</sup> The 'basal' concentration of noradrenaline at the cardiac neuroeffector junction is also unknown, but it is likely to be similar to circulating concentrations of noradrenaline, which are reportedly very low (1–2 nM).<sup>60</sup> Since the IC<sub>50</sub> for inhibition of  $I_{Kss}$  by noradrenaline was ~0.90 nM, it seems likely that this current would be inhibited, contributing to AP prolongation at relatively modest levels of sympathetic activity. On the other hand, this TREK-like channel current is activated by stretch and may make a greater contribution to AP repolarization under physiological mechanical loads *in vivo*.<sup>22</sup> The inhibition by noradrenaline may provide a mechanism by which AP configuration is optimized to mechanical load and degree of autonomic activation.

### 4.5 Limitations

This study provides good evidence of a role for a TREK-like  $I_{Kss}$  in repolarization of rat atrial myocytes and demonstrates the existence of a similar noradrenaline-sensitive current in mouse atrial cells. Expression of TREK-1 has recently been demonstrated in the human heart.<sup>61</sup>

However, it is currently unclear to what extent  $I_{Kss}$  contributes to the repolarization of the human atrium. Moreover, it is not clear whether these TREK-like currents are atrial selective. Further work is therefore merited to establish the contribution of  $I_{Kss}$  and  $K_{2P}$  channels to human cardiac electrophysiology.

## Supplementary material

Supplementary material is available at *Cardiovascular Research* online.

## Acknowledgements

We thank Clive Orchard (Bristol) and Eamonn Kelly (Bristol) for useful discussion.

**Conflict of interest:** R.B. was in receipt of a fellowship from the *British Heart Foundation* that funded this work (FS/10/68). A.F.J. and J.C.H. were lead applicants on the fellowship that funded this work (FS/10/68) and were principal investigators on the project grant that funded S.C.M.C. (PG/11/97). A.F.J. was a principal investigator on the project grant that funded S.M.B. (PG/10/91).

## Funding

This work was supported by the British Heart Foundation (FS/10/68 to R.B., PG/11/97 to S.C.M.C., and PG/10/91 to S.M.B.). Funding to pay the Open Access publication charges for this article was provided by the British Heart Foundation.

## References

- Volders PGA. Novel insights into the role of the sympathetic nervous system in cardiac arrhythmogenesis. *Heart Rhythm* 2010;**7**:1900–1906.
- Workman A. Cardiac adrenergic control and atrial fibrillation. *Naunyn Schmiedeberg's Arch Pharmacol* 2010;**381**:235–249.
- Xiao R-P, Zhu W, Zheng M, Cao C, Zhang Y, Lakatta EG, Han Q. Subtype-specific  $\alpha_1$ - and  $\beta$ -adrenoceptor signaling in the heart. *Trends Pharmacol Sci* 2006;**27**:330–337.
- Bers DM. Calcium cycling and signaling in cardiac myocytes. *Ann Rev Physiol* 2008;**70**:23–49.
- ter Keurs HEDJ, Boyden PA. Calcium and arrhythmogenesis. *Physiol Rev* 2007;**87**:457–506.
- Ravens U, Wang X-L, Wettwer E. Alpha adrenoceptor stimulation reduces outward currents in rat ventricular myocytes. *J Pharmacol Exp Therap* 1989;**250**:364–370.
- Fedida D, Braun AP, Giles WR.  $\alpha_1$ -Adrenoceptors reduce background  $K^+$  current in rabbit ventricular myocytes. *J Physiol (Lond)* 1991;**441**:673–684.
- Braun AP, Fedida D, Giles WR. Activation of  $\alpha_1$ -adrenoceptors modulates the inwardly rectifying potassium currents of mammalian atrial myocytes. *Pflügers Arch* 1992;**421**:431–439.
- Koumi S, Backer CL, Arentzen CE, Sato R. Beta-adrenergic modulation of the inwardly rectifying potassium channel in isolated human ventricular myocytes. Alteration in channel response to beta-adrenergic stimulation in failing human hearts. *J Clin Invest* 1995;**96**:2870–2881.
- Koumi S, Wasserstrom JA, Ten Eick RE.  $\beta$ -Adrenergic and cholinergic modulation of the inwardly rectifying  $K^+$  current in guinea-pig ventricular myocytes. *J Physiol (Lond)* 1995;**486**:647–659.
- Sato R, Koumi S. Modulation of the inwardly rectifying  $K^+$  channel in isolated human atrial myocytes by alpha-1-adrenergic stimulation. *J Memb Biol* 1995;**148**:185–191.
- Scamps F. Characterization of a beta-adrenergically inhibited  $K^+$  current in rat cardiac ventricular cells. *J Physiol (Lond)* 1996;**491**:81–97.
- Wang H, Yang B, Zhang Y, Han H, Wang J, Shi H, Wang Z. Different subtypes of alpha 1-adrenoceptor modulate different  $K^+$  currents via different signaling pathways in canine ventricular myocytes. *J Biol Chem* 2001;**276**:40811–40816.
- Choisy SC, Hancox JC, Arberr LA, Reynolds AM, Shattock MJ, James AF. Evidence for a novel  $K^+$  channel modulated by  $\alpha_{1A}$ -adrenoceptors in cardiac myocytes. *Mol Pharmacol* 2004;**66**:735–748.
- Nattel S, Yue L, Wang Z. Cardiac ultrarapid delayed rectifiers: a novel potassium current family of functional similarity and molecular diversity. *Cell Physiol Biochem* 1999;**9**:217–226.
- Hibino H, Inanobe A, Furutani K, Murakami S, Findlay I, Kurachi Y. Inwardly rectifying potassium channels: their structure, function, and physiological roles. *Physiol Rev* 2010;**90**:291–366.

17. Liu W, Saint DA. Heterogeneous expression of tandem-pore K<sup>+</sup> channel genes in adult and embryonic rat heart quantified by real-time polymerase chain reaction. *Clin Exp Pharmacol Physiol* 2004;**31**:174–178.
18. Tamargo J, Caballero R, Gomez R, Valenzuela C, Delpon E. Pharmacology of cardiac potassium channels. *Cardiovasc Res* 2004;**62**:9–33.
19. Ravens U, Wettwer E. Ultra-rapid delayed rectifier channels: molecular basis and therapeutic implications. *Cardiovasc Res* 2011;**89**:776–785.
20. Aimond F, Rauzier J-M, Bony C, Vassort G. Simultaneous activation of p38 MAPK and p42/44 MAPK by ATP stimulates the K<sup>+</sup> current I<sub>TREK</sub> in cardiomyocytes. *J Biol Chem* 2000;**275**:39110–39116.
21. Terrenoire C, Lauritzen I, Lesage F, Romey G, Lazdunski M. A TREK-1-like potassium channel in atrial cells inhibited by β-adrenergic stimulation and activated by volatile anesthetics. *Circ Res* 2001;**89**:336–342.
22. Li XT, Dyachenko V, Zuzarte M, Putzke C, Preisig-Muller R, Isenberg G, Daut J. The stretch-activated potassium channel TREK-1 in rat cardiac ventricular muscle. *Cardiovasc Res* 2006;**69**:86–97.
23. Stones R, Calaghan SC, Billeter R, Harrison SM, White E. Transmural variations in gene expression of stretch-modulated proteins in the rat left ventricle. *Pflügers Arch* 2007;**454**:545–549.
24. Zhang H, Shepherd N, Creazzo TL. Temperature-sensitive TREK currents contribute to setting the resting membrane potential in embryonic atrial myocytes. *J Physiol (Lond)* 2008;**586**:3645–3656.
25. Kim Y, Bang H, Kim D. TBAK-1 and TASK-1, two-pore K<sup>+</sup> channel subunits: kinetic properties and expression in rat heart. *Am J Physiol* 1999;**277**:H1669–H1678.
26. James AF, Ramsey JE, Reynolds AM, Hendry BM, Shattock MJ. Effects of endothelin-1 on K<sup>+</sup> currents from rat ventricular myocytes. *Biochem Biophys Res Commun* 2001;**284**:1048–1055.
27. Jones SA, Morton MJ, Hunter M, Boyett MR. Expression of TASK-1, a pH-sensitive twin-pore domain K<sup>+</sup> channel, in rat myocytes. *Am J Physiol* 2002;**283**:H181–H185.
28. Putzke C, Wemhöner K, Sachse FB, Rinné S, Schlichthörl G, Li XT, Jaé L, Eckhardt I, Wischmeyer E, Wulf H, Preisig-Müller R, Daut J, Decher N. The acid-sensitive potassium channel TASK-1 in rat cardiac muscle. *Cardiovasc Res* 2007;**75**:59–68.
29. Limberg SH, Netter MF, Rolfes C, Rinné S, Schlichthörl G, Zuzarte M, Vassiliou T, Moosdorf R, Wulf H, Daut J, Sachse F, Decher N. TASK-1 channels may modulate action potential duration of human atrial cardiomyocytes. *Cell Physiol Biochem* 2011;**28**:613–624.
30. Schiekel J, Lindner M, Hetzel A, Wemhöner K, Renigunta V, Schlichthörl G, Decher N, Oliver D, Daut J. Inhibition of the potassium channel TASK-1 in rat cardiac muscle by endothelin-1 is mediated by phospholipase C. *Cardiovasc Res* 2013;**97**:97–105.
31. Bhattacharjee A, Joiner WJ, Wu M, Yang Y, Sigworth FJ, Kaczmarek LK. Slick (Slo2.1), a rapidly-gating sodium-activated potassium channel inhibited by ATP. *J Neurosci* 2003;**23**:11681–11691.
32. Choisy SCM, Arberry LA, Hancox JC, James AF. Increased susceptibility to atrial tachyarrhythmia in spontaneously hypertensive rat hearts. *Hypertension* 2007;**49**:498–505.
33. Smith C, Teitler M. Beta-blocker selectivity at cloned human beta1- and beta2-adrenergic receptors. *Cardiovasc Drugs Therap* 1999;**13**:123–126.
34. Juberg EN, Minneman KP, Abel PW. β-Adrenoceptor binding and functional response in right and left atria of rat heart. *Naunyn Schmiedebergs Arch Pharmacol* 1985;**330**:193–202.
35. Hool LC, Harvey RD. Role of beta 1- and beta 2-adrenergic receptors in regulation of Cl<sup>-</sup> and Ca<sup>2+</sup> channels in guinea pig ventricular myocytes. *Am J Physiol* 1997;**273**:H1669–H1676.
36. Chase A, Colyer J, Orchard CH. Localised Ca channel phosphorylation modulates the distribution of L-type Ca current in cardiac myocytes. *J Mol Cell Cardiol* 2010;**49**:121–131.
37. Yan D-H, Nishimura K, Yoshida K, Nakahira K, Ehara T, Igarashi K, Ishihara K. Different intracellular polyamine concentrations underlie the difference in the inward rectifier K<sup>+</sup> currents in atria and ventricles of the guinea-pig heart. *J Physiol (Lond)* 2005;**563**:713–724.
38. Neher E, Stevens CF. Conductance fluctuations and ionic pores in membranes. *Ann Rev Biophys Bioeng* 1977;**6**:345–381.
39. Pongs O. Molecular biology of voltage-dependent potassium channels. *Physiol Rev* 1992;**72**:S69–S88.
40. Knollmann BC, Sirenko S, Rong Q, Katchman AN, Casimiro M, Pfeifer K, Ebert SN. Kcnq1 contributes to an adrenergic-sensitive steady-state K<sup>+</sup> current in mouse heart. *Biochem Biophys Res Commun* 2007;**360**:212–218.
41. Leonoudakis D, Gray AT, Winegar BD, Kindler CH, Harada M, Taylor DM, Chavez RA, Forsayeth JR, Yost CS. An open rectifier potassium channel with two pore domains in tandem cloned from rat cerebellum. *J Neurosci* 1998;**18**:868–878.
42. Clarke CE, Veale EL, Green PJ, Meadows HJ, Mathie A. Selective block of the human 2-P domain potassium channel, TASK-3, and the native leak potassium current, I<sub>KSO</sub>, by zinc. *J Physiol (Lond)* 2004;**560**:51–62.
43. Enyeart JJ, Xu L, Danthi S, Enyeart JA. An ACTH- and ATP-regulated background K<sup>+</sup> channel in adrenocortical cells is TREK-1. *J Biol Chem* 2002;**277**:49186–49199.
44. Kennard LE, Chumbley JR, Ranatunga KM, Armstrong SJ, Veale EL, Mathie A. Inhibition of the human two-pore domain potassium channel, TREK-1, by fluoxetine and its metabolite norfluoxetine. *Br J Pharmacol* 2005;**144**:284–289.
45. Czirájk G, Enyedi P. Zinc and mercuric ions distinguish TREK from the other two-pore-domain K<sup>+</sup> channels. *Mol Pharmacol* 2006;**69**:1024–1032.
46. Thümmler S, Duprat F, Lazdunski M. Antipsychotics inhibit TREK but not TRAAK channels. *Biochem Biophys Res Commun* 2007;**354**:284–289.
47. Patel AJ, Honore E, Maingret F, Lesage F, Fink M, Duprat F, Lazdunski M. A mammalian two pore domain mechano-gated S-like K<sup>+</sup> channel. *EMBO J* 1998;**17**:4283–4290.
48. Fink M, Duprat F, Lesage F, Reyes R, Romey G, Heurteaux C, Lazdunski M. Cloning, functional expression and brain localization of a novel unconventional outward rectifier K<sup>+</sup> channel. *EMBO J* 1996;**15**:6854–6862.
49. Enyedi P, Czirájk G. Molecular background of leak K<sup>+</sup> currents: two-pore domain potassium channels. *Physiol Rev* 2010;**90**:559–605.
50. Ma X-Y, Yu J-M, Zhang S-Z, Liu X-Y, Wu B-H, Wei X-L, Yan J-Q, Sun H-L, Yan H-T, Zheng J-Q. External Ba<sup>2+</sup> block of the two-pore domain potassium channel TREK-1 defines conformational transition in its selectivity filter. *J Biol Chem* 2011;**286**:39813–39822.
51. Frielle T, Daniel KW, Caron MG, Lefkowitz RJ. Structural basis of beta-adrenergic receptor subtype specificity studied with chimeric beta 1/beta 2-adrenergic receptors. *Proc Natl Acad Sci USA* 1988;**85**:9494–9498.
52. Hoffmann C, Leitz MR, Oberdorf-Maass S, Lohse MJ, Klotz KN. Comparative pharmacology of human β-adrenergic receptor subtypes—characterization of stably transfected receptors in CHO cells. *Naunyn Schmiedebergs Arch Pharmacol* 2004;**369**:151–159.
53. Baker JG. The selectivity of β-adrenoceptor agonists at human β<sub>1</sub>-, β<sub>2</sub>- and β<sub>3</sub>-adrenoceptors. *Br J Pharmacol* 2010;**160**:1048–1061.
54. Zhu W-Z, Chakir K, Zhang S, Yang D, Lavoie C, Bouvier M, Hébert TE, Lakatta EG, Cheng H, Xiao R-P. Heterodimerization of β<sub>1</sub>- and β<sub>2</sub>-adrenergic receptor subtypes optimizes β-adrenergic modulation of cardiac contractility. *Circ Res* 2005;**97**:244–251.
55. Belevych AE, Juranek I, Harvey RD. Protein kinase C regulates functional coupling of β<sub>1</sub>-adrenergic receptors to G<sub>i/o</sub>-mediated responses in cardiac myocytes. *FASEB J* 2004;**18**:367–369.
56. Harvey RD, Hell JW. CaV1.2 signaling complexes in the heart. *J Mol Cell Cardiol* 2013;**58**:143–152.
57. Murray AJ. Pharmacological PKA inhibition: all may not be what it seems. *Sci Signal* 2008;**1**:re4.
58. Trafford AW, Clarke JD, Eisner DA, Dibb KM. Calcium signalling microdomains and the t-tubular system in atrial myocytes: potential roles in cardiac disease and arrhythmias. *Cardiovasc Res* 2013;**98**:192–203.
59. Bryant S, Kimura TE, Kong CHT, Watson JJ, Chase A, Suleiman MS, James AF, Orchard CH. Stimulation of I<sub>Ca</sub> by basal PKA activity is facilitated by caveolin-3 in cardiac ventricular myocytes. *J Mol Cell Cardiol* 2014;**68**:47–55.
60. Goldstein DS, McCarty R, Polinsky RJ, Kopin JJ. Relationship between plasma norepinephrine and sympathetic neural activity. *Hypertension* 1983;**5**:552–559.
61. Hund TJ, Snyder JS, Wu X, Glynn P, Koval OM, Onal B, Leymaster ND, Unudurthi SD, Curran J, Camardo C, Wright PJ, Binkley PF, Anderson ME, Mohler PJ. β<sub>1V</sub>-Spectrin regulates TREK-1 membrane targeting in the heart. *Cardiovasc Res* 2014;**102**:166–175.